Proceedings of the 19th International Symposium on the
Packaging and Transportation of Radioactive Materials
PATRAM 2019
August 4-9, 2019, New Orleans, LA, USA

COMPOSITION AND EVOLUTION OF SEA-SALT DELIQUESCENT BRINES ON SNF STORAGE CANISTER SURFACES

Charles Bryan
Sandia National Laboratories
Albuquerque, NM 87185
U.S.A.

Eric Schindelholz
Sandia National Laboratories
Albuquerque, NM 87185
U.S.A

Andrew Knight
Sandia National Laboratories
Albuquerque, NM 87185
U.S.A.

Jason Taylor
Sandia National Laboratories
Albuquerque, NM 87185
U.S.A

ABSTRACT

For long-term storage, spent nuclear fuel (SNF) is placed in dry storage systems, commonly consisting of welded stainless steel containers enclosed in ventilated cement or steel overpacks. At near-marine sites, a significant fraction of aerosols deposited on the canisters may be sea-salts, which as the canister cools, will deliquesce to form chloride rich brines, potentially leading to chloride-induced stress corrosion cracking (SCC). Here, we have used thermodynamic modeling to predict the evolving composition of sea-salt deliquescent brines as the canisters cool and the surface relative humidity increases. Representative brine compositions have been mixed, and we have characterized their physical and electrochemical properties, including density, viscosity, conductivity, and oxygen concentrations. These parameters are necessary for predicting the corrosion behavior of the storage canisters over time.

When predicting corrosion behavior, it is common to assume that sea-salt brines form and persist unchanged over time. However, here we show that the magnesium chloride rich-brines that form when sea-salt aerosols initially deliquesce are not stable at elevated temperatures. Elevated temperatures increase brine $HCl_{(g)}$ partial pressures, driving chloride loss through degassing of HCl. Concomitantly, pH rises until precipitation of less-deliquescent phases such as magnesium carbonate and magnesium hydroxy-chloride. These reactions buffer the pH, allowing continued degassing of chloride; ultimately, complete brine dry-out may occur. In the absence of magnesium chloride, the remaining sea-salts will not deliquesce until temperatures cool further, allowing higher RH values on the canister surface. These data suggest that initiation of corrosion may be delayed for longer than previously thought.

INTRODUCTION

In the United States, spent nuclear fuel (SNF) from nuclear power reactors is eventually moved from storage pools to dry storage at near-reactor Independent Spent Fuel Storage Installations (ISFSIs). Typically, the dry storage systems are welded stainless steel (304 SS or 316 SS) containers enclosed in concrete, or steel and concrete, overpacks[1]. For most dry storage systems, passive ventilation is used to cool the canisters within the overpacks, and large volumes of outside air are drawn through the system by natural convection. Dust and aerosols within the air are deposited on the steel canisters, and, as the casks cool over time, salts in the dust will deliquesce (absorb water) to form brine on the storage container surface. If the salts contain aggressive components such as chloride, localized attack can occur. One corrosion mechanism, chloride-induced stress corrosion cracking (SCC), may propagate relatively rapidly under some conditions and potentially result in canister penetration during long-term interim storage. Chloride-induced SCC is a well-documented mode of attack for stainless steels in marine environments[2], and many ISFSIs are in coastal areas. Sea-salt aerosols have been observed in dust samples collected from canister surfaces at the Diablo Canyon ISFSI[3,4].

Once corrosion can occur, brine layer properties control the distribution and size of the cathode around a corrosion pit and limit the maximum cathodic current that can be produced[5], thus affecting corrosion kinetics, damage distributions, and the extent of corrosion (e.g., maximum pit depth) on the metal surface. Pitting initiation and growth will in turn affect the timing of SCC crack initiation[6,7]. The brine properties (volume, composition, and electrochemical properties) change over time as deposited salt loads increase and the canister continues to cool, resulting in a rise in the relative humidity (RH) at the canister surface. Understanding the brine evolution as a function of the changing RH, temperature, and salt load is necessary to develop improved predictive models for long-term canister corrosion performance.

We have used standard thermodynamic modeling to determine the composition of brines formed by sea-salt deliquescence, as a function of RH and temperature; and then mixed brines to represent specific RH values and characterized those brines, measuring conductivity, density, and viscosity; oxygen contents were also measured, to verify values predicted by the thermodynamic model. The theoretical and experimental data were used to calculate brine volumes and brine-to-salt volume ratios as a function of RH and salt load. These data provide insights into structure and composition of deliquescent brines and the potential limits on the extent of atmospheric corrosion on heated metal surfaces.

Additional reactions that must be considered are reactions with atmospheric components that may affect its composition and volume. Here we show that at elevated temperatures, the magnesium chloride-rich brines that form first when sea-salts deliquesce generate high partial pressures of HCl gas and degas, precipitating non-deliquescent phases. In the absence of magnesium chloride, the remaining sea-salts will not deliquesce until temperatures cool further, and higher RH values are achieved on the canister surface.

THERMODYNAMIC MODELING OF SEA-SALT DELIQUESCENT BRINES

Sea-salt aerosols reflect the composition of sea water. Dominant ions in seawater are Na^+ and Cl^- with lesser amounts of Mg^{2+}, Ca^{2+}, K^+, and SO_4^{2-}. Sea spray evaporates to form more and more concentrated solutions, eventually converting to dry salts. These salts, upon deliquescence, follow the evaporation pathway in reverse, initially forming highly concentrated magnesium chloride-rich brines, and progressively become more and more dilute. At equilibrium, the activity of water (a_w)

in a brine is equal to the activity of water in the atmosphere above the brine, which is equal to the RH, expressed as a unit value. Hence, by modeling the evolution of seawater as it evaporates, the deliquescent brine compositions can be calculated. The compositional evolution of evaporating seawater has been modeled using the thermodynamic solubility and speciation modeling program EQ3/6[8] and the Yucca Mountain Program Pitzer database[9]; these calculations are described in detail in Bryan and Schindelholz[10] and are only summarized here. ASTM substitute seawater[11], which is based on an average seawater composition, was used as the starting composition for the calculation.

Model predictions for seawater evaporation at 25ºC are shown in Figure 1. In Figure 1a, solute concentrations are plotted against RH (a_w × 100). In Figure 1b, the concentrations are given in terms of concentration factor (CF), calculated as (original water mass)/(remaining water mass). During evaporation, brines are dominantly Na+ and Cl^- rich until halite precipitates at 74% RH (CF of 11), and then evolve towards Mg^{2+}-Cl^- brines until bischofite ($MgCl_2$:$6H_2O$) precipitates at 36% RH (CF of 222); at this point, the brine is almost entirely $MgCl_2$. Predicted brine compositions below this point are speculative, as they are outside the range of model validation.

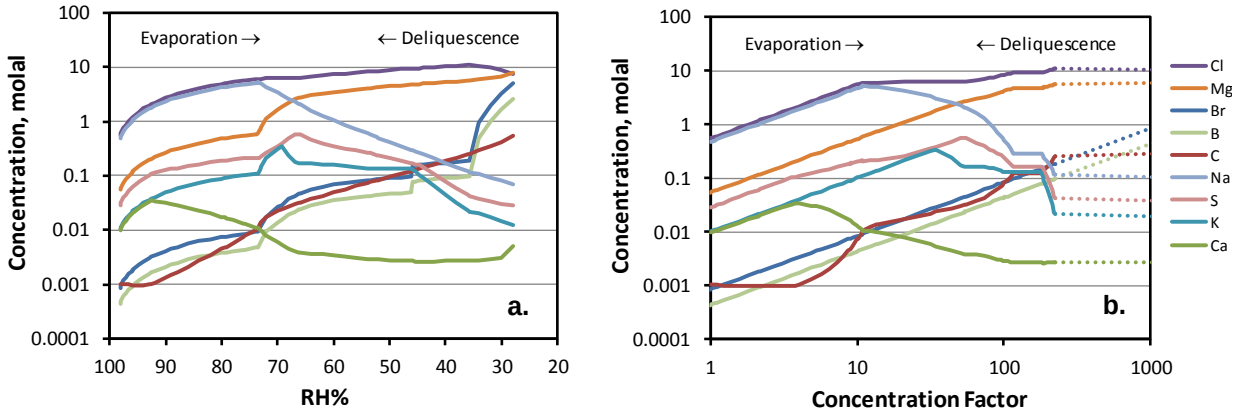

Figure 1: Evaporation of seawater. (a) Predicted brine composition as a function of RH. (b) Predicted brine composition as a function of concentration factor.

Salt minerals that are predicted to precipitate in order of occurrence, are as follows: calcite ($CaCO_3$) precipitates first, and then gypsum ($CaSO_4$:$2H_2O$), which converts to anhydrite ($CaSO_4$) at a concentration factor of about 9. Halite (NaCl) precipitates at a concentration factor of about 11. Other minerals precipitate, and in many cases re-dissolve, as the seawater evaporates. The final salt assemblage at dry-out consists mostly of halite, with minor amounts of bischofite ($MgCl_2$:$6H_2O$) and kieserite ($MgSO_4$:$2H_2O$) and trace amounts of anhydrite, carnallite ($KMgCl_2$:$6H_2O$), and hydromagnesite ($Mg_5(CO_3)_4(OH)_2$:$4H_2O$). As sea-spray aerosols dry out, these salts are precipitated, and salts, or a mixture of salts and brine, may be deposited on the canister surface. As the canisters cool and the RH rises, the salts re-dissolve and the composition of the deliquescent brine follows the path of evaporation in reverse order. It is the highly deliquescent $MgCl_2$:$6H_2O$ that is believed to control the deliquescence behavior of sea salts, determining when an aqueous phase is present.

The data in Figure 1 are for seawater evaporation at 25ºC, but evaporation was modeled at temperatures from 10ºC to 80ºC, and the predicted brine compositions do not vary greatly. The largest effect of temperature is on the deliquescence point of bischofite, which shifts from 36% to

28% RH at the highest temperature. The deliquescence point of halite at ~74% RH is nearly independent of temperature.

As sea-salts deliquesce, the volume of brine present changes. Using the thermodynamic modeling results and brine densities estimated from measured values, the volume of the brine has been calculated as a function of RH and surface salt load. By assuming that the brine is distributed as a uniform film across the surface, a brine film thickness has been calculated. Since salt aerosols are deposited across the surface as discrete particles, this assumption is a simplification, especially at low salt loads. However, the estimated thicknesses provide insights into the potential importance of corrosion processes dependent upon brine film thickness.

Figure 2a shows predicted brine layer thicknesses at 25ºC as a function of RH and surface salt load (given in units of grams of chloride, as sea salt, per meter squared); Figure 2b shows the dependence on temperature. Predicted brine layer thicknesses for each salt load form parallel trends as a function of RH because brine layer thicknesses vary linearly with salt load. Inflections in each curve represent conditions at which a salt mineral precipitates. For each surface load, the layer thickness decreases by about a factor of 10 as the RH is reduced from 98% (unevaporated sea-water) to 74%, when NaCl precipitates. Thicknesses decreases an additional order of magnitude as the RH drops to about 46%, where carnallite precipitates. At lower RH values, the brine is nearly pure magnesium chloride, until bischofite precipitates at 36% RH (at 25ºC). An important observation is that once corrosion begins, oxygen diffusion through the brine layer is not anticipated to be limiting with respect to the oxygen reduction reaction for brine films thinner than 20 µm[12], and calculated brine layer thicknesses below the deliquescence point of NaCl are consistently thinner than that, even for relatively high salt loads.

The relative volume of brine present was calculated from the thermodynamic data, known mineral densities. and measured brine densities (Figure 3). This information is useful in assessing the degree of continuity in the brine layer that might form by deliquescence of small (generally ~10 µm), isolated sea-salt aerosols. At RH values above the deliquescence point of NaCl, brine volumes are orders of magnitude greater than the precipitated salt volumes, which consist only of small amounts of calcite and gypsum. At RH values below 74%, brine volumes decrease rapidly as NaCl precipitates. At 60% RH, brine and precipitated salts are about equal in volume. At the point of bischofite deliquescence, the brine volume about 1/3 the volume of the solids.

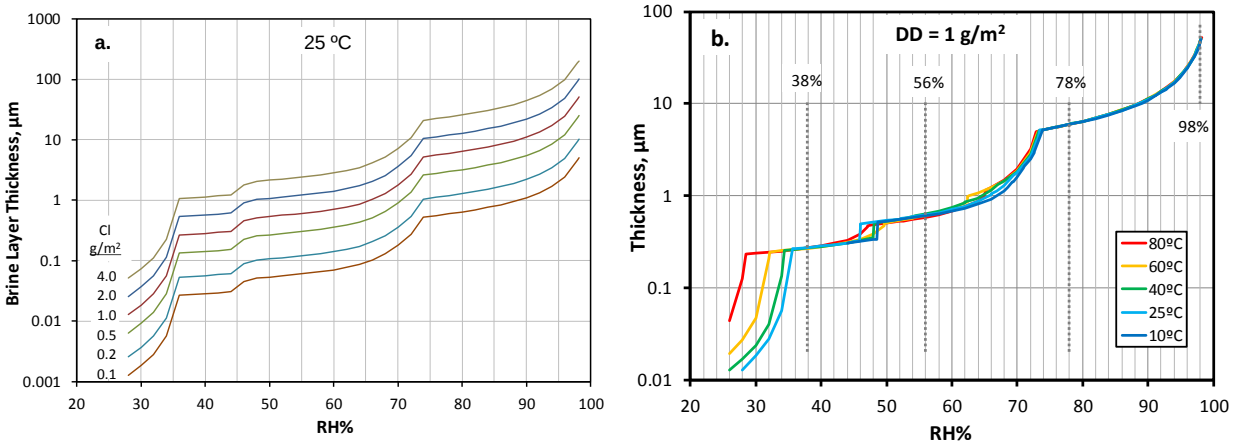

Figure 2. Calculated brine layer thicknesses, as a function of RH and (a) salt load (grams chloride/m^2), and (b) temperature.

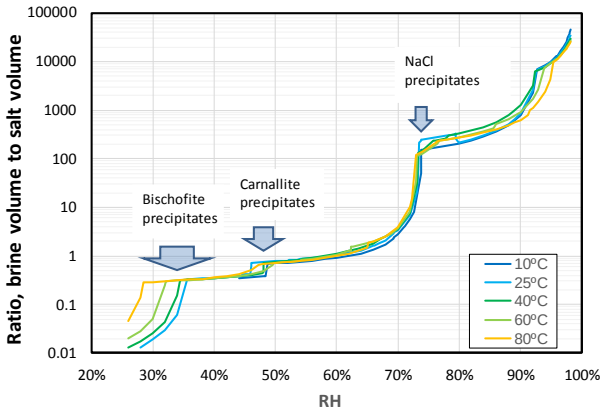

Figure 3. Variation in brine/salt volume ratio with RH.

EXPERIMENTAL MEASUREMENT OF BRINE PROPERTIES

Important brine properties that are necessary for mechanistic pitting models[5] are brine volume, (requiring brine density be known), conductivity, oxygen content, and viscosity. To estimate these values, several brine compositions along the predicted evolutionary pathway for seawater evaporation at 25ºC were mixed using ACS certified salts, and these properties were measured experimentally. The brines correspond to the predicted compositions at RH values of 98.15% (unevaporated seawater), 90%, 78%, 73.4%, 66%, 56%, and 38%. Once mixed, conductivity was measured using a Jenway Model 4510 Conductivity Meter with high ionic strength conductivity probes. Solution densities were measured using hydrometers calibrated for specific gravity ranges from 1.000 to 1.220, and 1.20 to 1.420. Hydrometer accuracy at temperatures above their calibration temperature were verified by measuring the density of saturated NaCl solutions at the temperatures of interest[13]. Viscosities were measured over the temperature range from 20º to 60ºC using a Brookfield AMETEK LDTV2T Viscometer with a low viscosity adaptor. Finally, oxygen concentrations were measured at selected temperatures to verify predictions from the thermodynamic model using iodometric titration[14].

For each brine, conductivities were measured for a range from <25ºC to >60ºC; measured conductivities varied linearly as a function of temperature, so these data were used to estimate brine conductivities from 10ºC to 80ºC (Figure 4a). While solution concentrations (ionic strength) increases consistently as the RH decreases, conductivity shows a more complex response. At high RH (e.g., seawater), ionic strength and conductivity are both low. As the RH drops and the solution becomes more concentrated, the conductivity increases, reaching a maximum at the point of halite deliquescence, when the solution concentration is approximately 6 molal sodium chloride. As the RH decreases further, the brine becomes more and more magnesium-rich and the conductivity drops; this is consistent with anticipated behavior of divalent cation-rich brines[15]. Measured brine densities for temperatures up to 65ºC are shown in Figure 4b. Brine densities decrease with temperature, but the change is small. Brine viscosities are shown in Figure 4c. Measured oxygen concentrations are shown in Figure 4d, and were evaluated to verify thermodynamic model predictions, also shown. Measured oxygen concentrations correspond well for low temperature solutions over the entire RH range, and for more dilute (higher RH) higher temperatures solutions; however, method limitations did not permit accurate analysis for the most concentrated brines at the highest temperatures studied (60ºC and 80ºC). Viscosity and oxygen concentration are used for estimating the maximum cathodic current that can support pit growth during active corrosion.

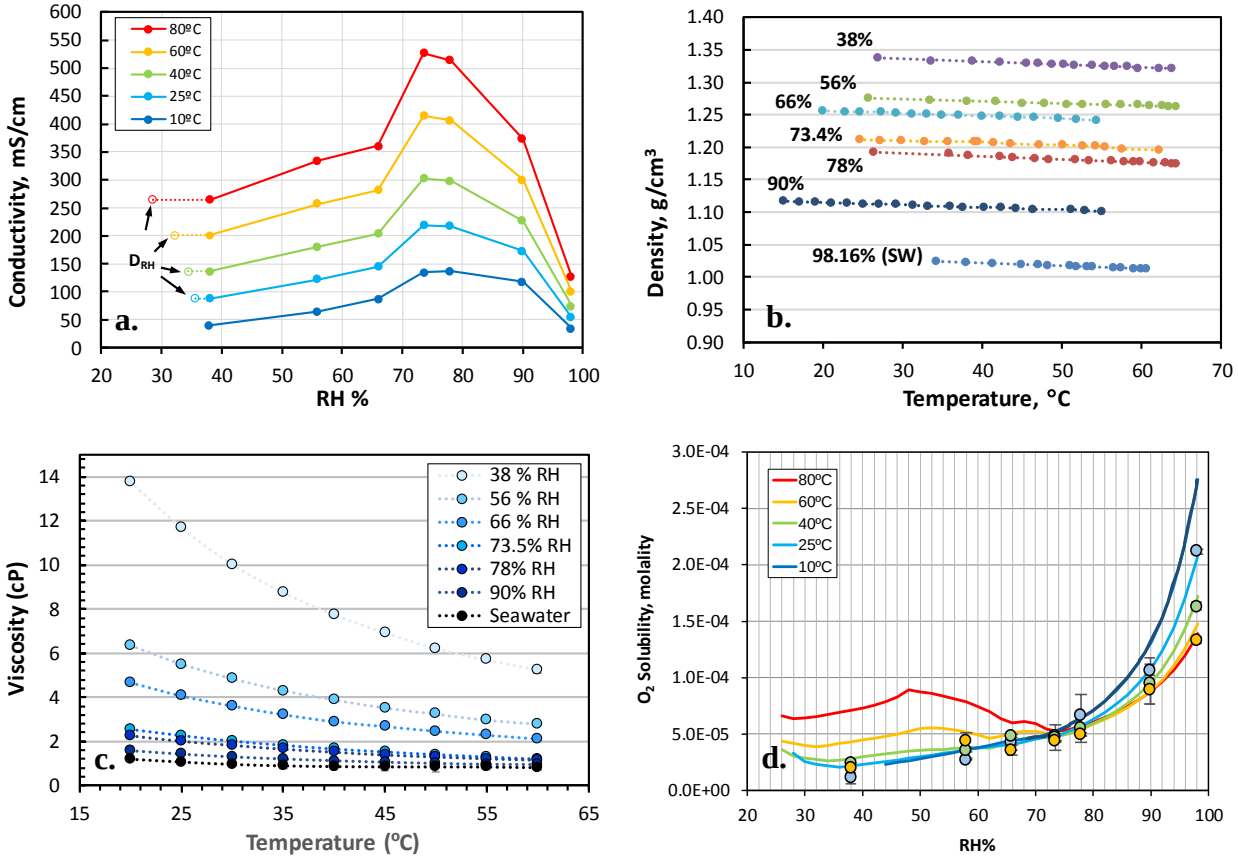

Figure 4. Measured properties of representative sea-salt brines (a) conductivity; (b) density; (c) viscosity; (d) oxygen content (measured and calculated).

BRINE STABILITY ON HEATED CANISTER SURFACES

The brine compositions and precipitated salt assemblages predicted here represent evaporation of seawater or deliquescence of sea-salts in bulk amounts and at relatively low temperatures, and equilibrium with atmospheric gases present at constant and relatively high levels (O_2, CO_2) is assumed. However, any chloride-containing brine will generate a partial pressure of HCl, and if that partial pressure is greater than the partial pressure of the HCl in the atmosphere, then that brine will degas HCl. For bulk systems, reactions that can result in degassing of HCl can be ignored, the partial pressures of HCl that are generated are extremely low, so that a huge volume of air is necessary to sweep away any significant amount of chloride. For sea-salt aerosols, HCl degassing cannot be ignored, because the total amount of chloride present is very small and surface areas for exchange with the atmosphere are very large. Moreover, several reactions with atmospheric gases can buffer the pH, allowing for continued degassing of HCl. These include sea-salt aerosol reactions with strong inorganic acids such as HNO_3 and SO_2 (which reacts with water to form H_2SO_4). In addition, there are a number of photochemically-mediated reactions with nitrous oxides that can transfer chloride from the solid to the gas phase. The importance of such reactions is strongly site-specific, as HNO_3 and SO_2 levels in the atmosphere vary widely.

With partially deliquesced sea-salts in contact with a magnesium-rich brine, a similar reaction can occur with CO_2, which acts as a weak acid, forming carbonic acid in solution. As CO_2 is absorbed

and HCl degasses, the pH continues to rise until a carbonate mineral precipitates. At that point, the pH is buffered and the solution composition becomes invariant:

$$Mg^{+2}(aq) + 2Cl^{-}(aq) + H_2O + CO_2(g) \rightarrow MgCO_3(s) + 2HCl(g)$$

If this reaction goes to completion, then the highly deliquescent magnesium chloride is replaced with non-deliquescent magnesium carbonate and the sea-salt brine will dry out, narrowing the RH range over which metal corrosion can occur. Thermodynamic modeling (EQ3/6 and the Yucca Mountain Pitzer database) indicates that this reaction is strongly temperature-sensitive. At low temperatures, brine HCl partial pressures may be lower than ambient values, and HCl will be absorbed by the particles. At elevated temperatures, the brines degas HCl and absorb CO_2 to form the carbonate. The direction of the reaction is determined by the relative magnitudes of the ambient HCl partial pressure and that being generated by the brine at the pH at which it is buffered by magnesium carbonate precipitation. The modeling indicated that magnesium carbonate was the thermodynamically stable phase to precipitate, but if CO_2 absorption or carbonate formation was kinetically inhibited (allowing the pH to rise to a higher value), a magnesium hydroxy-chloride might precipitate. To assess the importance of these reactions, we performed two experiments. In each case, magnesium chloride brine was deposited as discrete droplets onto inert substrates (silicon wafers) and then placed into a controlled atmosphere chamber with an air flow rate of 2 L/minute, using air stripped of any acidic contaminants, but not of CO_2. The first experiment was carried out at 48ºC and 40% RH, approximately the maximum temperature conditions at which a magnesium chloride brine could deliquesce in actual canister storage conditions. The second was carried out at 85ºC and 35% RH. An RH this high is not achievable at 85ºC on a real, in-service canister; however, these conditions have been used for accelerated corrosion testing with sea-salts and magnesium chloride by these authors and others[16] and understanding the stability of brines under these conditions is required to interpret the experimental results. In both cases, samples were taken periodically over a period of about 8 weeks, and then analyzed using Scanning Electron Microscopy (SEM) and Energy Dispersive X-ray Spectroscopy (EDS), Time-of-Flight Secondary Ion Mass Spectrometry (TOF-SIMS), and Raman spectroscopy. Finally, except for the samples for TOF-SIMS analysis, all samples were leached with deionized water, and the dissolved salts were analyzed by ion chromatography (IC). This yielded Mg and Cl concentrations, but not carbonate.

After about 68 days of exposure, the 48ºC samples were examined by SEM-EDS. A secondary electron (SE) image of one sample is shown in Figure 5. The image shows the distribution of the brine on the silicon wafer, occurring as randomly located, but non-overlapping droplets, varying in size from 10-25 μm in diameter. Originally present as liquid droplets in the humidity chamber, the droplets dried in the vacuum of the SEM. Most droplets (80-90%), dried to leave a smooth but wrinkled, "raisin-like" surface. A fraction of the smaller droplets dried to form rings with elevated edges and smooth centers. Element maps of the region imaged are also shown in Figure 5 and illustrate that there is a strong compositional control on droplet morphology; the ring-like droplets contain carbon, while the more abundant wrinkled droplets do not. The relationship between composition and droplet morphology was confirmed by EDS X-ray analysis. The ring-like droplets still show large chloride peaks and only partially converted to carbonate. Magnesium carbonates are much less deliquescent than magnesium chloride and would not be deliquesced at 40% RH. Hence, as the conversion progressed, the volume of brine in the droplet decreased, resulting in the formation of a flatter droplet upon drying. Moreover, the conversion to carbonate

results in a large mass and volume loss in the dried salts, because the possible Mg-carbonates do not contain as much water as the bischofite.

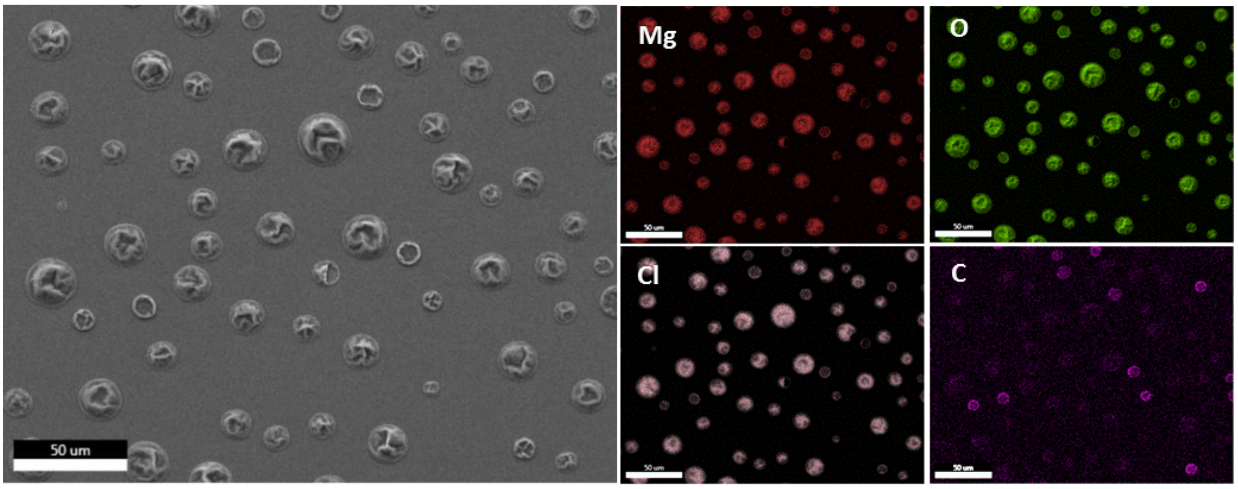

Figure 5. SEM image and element maps of magnesium chloride droplets exposed for 68 days at 48ºC and 40% RH, illustrating the relationship between droplet size and morphology, and composition.

Raman spectroscopic analysis of the sample confirmed that carbonate was present in small amounts. Leaching and chemical analysis of the salts present on the wafers showed that chloride was progressively lost during the experiment; however, to due to low air flow rates, conversion was not complete. After 8 weeks, only 5-7% of the total chloride had been lost. No such limitation is present for magnesium chloride on a canister surface, because canister heat generation drives advective airflow through the overpacks.

In the 85ºC experiment, considerably higher levels of chloride loss were observed. SEM/EDS analysis of the samples after 2, 4, and 8 weeks indicated progressive changes in droplet texture and loss of chloride, with smaller droplets being affected more than larger ones. This is illustrated in Figure 6 for one of the samples collected after 56 days. In the SEM backscattered electron image, smaller droplets are darker, indicating a lower average atomic number. This is consistent with chloride loss, as chlorine is the heaviest element in magnesium chloride. EDS element maps show that smaller droplets are strongly depleted in chloride and enriched in oxygen and in carbon (as carbonate) relative to the larger, less reacted droplets which still consist largely of bischofite, $MgCl_2{:}6H_2O$. These elemental distributions were confirmed by Time-of-Flight Secondary Ion Mass Spectroscopy. X-ray Diffraction analysis indicated the material on the wafers was dominantly bischofite, but also identified a small amount of a magnesium hydroxy-chloride, $Mg_3(OH)_4Cl_2{:}4H_2O$. Hence, via HCl degassing, some of the originally deposited magnesium chloride brine (Mg:Cl = 1:2) had converted the less deliquescent hydroxy-chloride (Mg:Cl = 3/2). As with the previous experiment, air flow was insufficient to support conversion of all the magnesium chloride over the course of the experiment.

These two experiments demonstrate the relative instability of magnesium chloride brines at elevated temperatures. Under both field and laboratory conditions, $MgCl_2$ brine at elevated temperatures can react with atmospheric CO_2 to degas HCl, converting to non-deliquescent magnesium carbonate or hydroxy-chlorides; if taken to completion, the brines could dry out,

eliminating the aqueous phase on the canister surface and delaying corrosion until temperatures drop sufficiently for other salt phases to deliquesce. It is also important to note that as SNF storage canisters cool and surface temperatures drop, the reaction could reverse—the magnesium carbonate could absorb HCl and form a chloride-rich brine again. Understanding the HCl degassing reactions described here is critically important in experimental systems, where elevated temperatures are frequently used to accelerate corrosion processes. Especially with experiments using sea-salts, where only a small fraction of the deposited salts is magnesium chloride, the possibility of carbonation and dry-out is real.

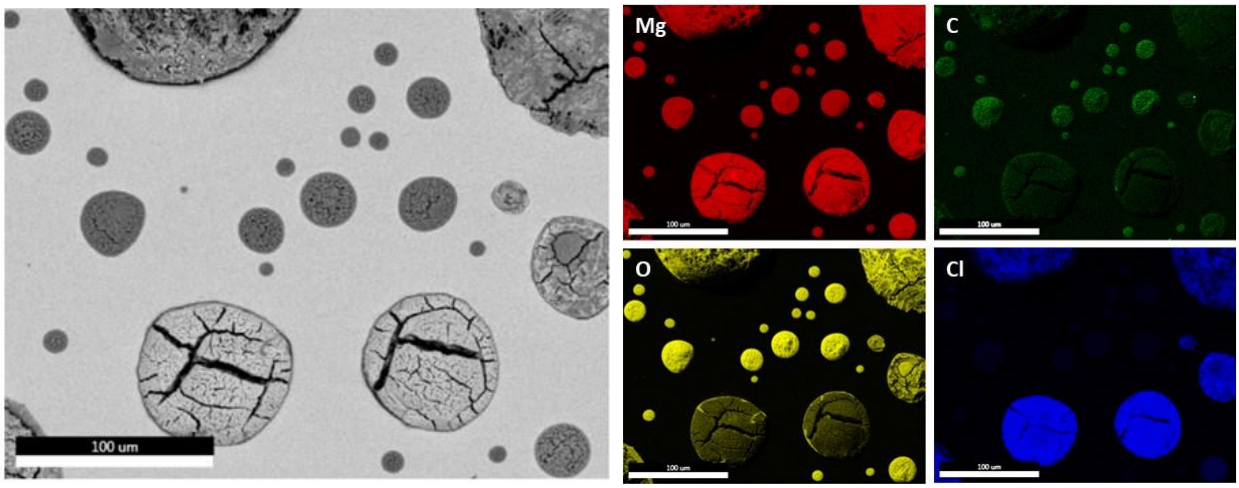

Figure 6. SEM image and element maps of magnesium chloride droplets on a sample exposed for 56 days at 85ºC and 35% RH, illustrating the relationship between droplet size and composition.

CONCLUSIONS

We have used thermodynamic modeling to predict the chemical composition of the brines that form by deliquescence of sea-salt aerosols, and to estimate brine volumes and salt/brine volume ratios as a function of temperature and atmospheric relative humidity. The brine volume calculations quantitatively illustrate that brines formed by deliquescence of sea-salt aerosols are unlikely to form by continuous films by deliquescence alone, although other forces may act to disperse the brines diffusion, capillary effects, etc.) on the metal surface. We have also mixed representative brines and measured the physical and electrochemical properties of those brines over a range of temperatures. Brine volumes and properties affect corrosion kinetics and damage distributions on the metal surface and may offer important constraints on the expected rate and extent of corrosion and the timing of SCC crack initiation.

We have experimentally evaluated the stability of magnesium chloride brines which form first upon sea-salt deliquescence and have shown that reactions leading to precipitation of carbonate or magnesium hydroxy-chloride are favored at elevated temperatures. These reactions may delay the occurrence of stable brines on the canister surfaces, until temperatures drop sufficiently to allow other salts to deliquesce. Moreover, consideration of these reactions is important in planning and interpreting laboratory corrosion experiments, that may be carried out for months or years within controlled-atmosphere chambers; and are frequently carried out under “accelerated” (high temperature) conditions that would favor brine degassing and conversion to non-deliquescent phases.

ACKNOWLEDGEMENTS

Sandia National Laboratories is a multimission laboratory managed and operated by National Technology and Engineering Solutions of Sandia, LLC., a wholly owned subsidiary of Honeywell International, Inc., for the U.S. Department of Energy's National Nuclear Security Administration under contract DE-NA0003525. Document # SAND2019-6151 C.

REFERENCES

1. B. Hanson, H. Alsaed, C. Stockman, D. Enos, D., R. Meyer, K. Sorenson, "Gap Analysis to Support Extended Storage of Used Nuclear Fuel" FCRD-USED-2011-000136 (U.S. Department of Energy, 2012): p. 218.
2. R.M. Kain, "Marine atmosphere corrosion cracking of austenitic stainless steels," *Materials Performance* 29,12 (1990): pp. 60-62.
3. C.R. Bryan, D.E. Enos, "Analysis of Dust Samples Collected from Spent Nuclear Fuel Interim Storage Containers at Hope Creek, Delaware, and Diablo Canyon, California" SAND2014-16383 (Albuquerque, NM, Sandia National Laboratories, 2014), p. 281.
4. EPRI, "Diablo Canyon Stainless Steel Dry Storage Canister Inspection" Technical Report #3002002822 (Palo Alto, CA, Electric Power Research Institute, 2016): p. 100.
5. Z. Chen, R. Kelly, "Computational modeling of bounding conditions for pit size on stainless steel in atmospheric environments," *Journal of the Electrochemical Society* 157, 2 (2010): pp. C69-C78.
6. Y. Kondo, "Prediction of fatigue crack initiation life based on pit growth," *Corrosion* 45, 1, (1989): pp. 7-11.
7. A. Turnbull, L. McCartney, S. Zhou, "A model to predict the evolution of pitting corrosion and the pit-to-crack transition incorporating statistically distributed input parameters," *Corrosion Science* 48, 8 (2006): pp. 2084-2105.
8. T.J. Wolery, *EQ3/6 A Software Package for Geochemical Modeling*, Lawrence Livermore National Lab, Livermore, CA (2010). https://www.osti.gov/servlets/purl/1231666
9. SNL. (2007). *In-drift precipitates/salts model*. ANL-EBS-MD-000045 REV 03. Sandia National Laboratories (2007): 358 p.
10. C.R. Bryan and E.J. Schindelholz, "Properties of Brines formed by Deliquescence of Sea-Salt Aerosols" Proceedings of 2018 NACE Corrosion Conf. (2018): Paper# C2018-10516.
11. ASTM D1141-98, "Standard Practice for the Preparation of Substitute Ocean Water" (West Conshohocken, PA: ASTM).
12. A. Nishikata, Y. Ichihara, Y. Hayashi, T. Tsuru, "Influence of electrolyte layer thickness and pH on the initial stage of the atmospheric corrosion of iron," *Journal of the Electrochemical Society* 144, 4 (1997): pp.1244-1252.
13. V.L. Thurmond, R.W. Potter, M.A. Clynne, "The Densities of Saturated Solutions of NaCl and KCl from 10ºC to 105ºC" U.S.G.S. Open File Report 84-253 (U.S. Geological Survey, 1984): p. 10.
14. L.S. Clesceri, A.E. Greenberg, and A.D. Eaton, *Standard methods for the examination of water and wastewater*, American Public Health Association. American Water Works Association and World Environment Federation. 20th Edition, Washington DC (1998).
15. J.O.M Bockris, A.K.N. Reddy, *Modern Electrochemistry: Ionics*. *2nd Edition*, (New York, NY: Kluwer Academic, 2002) p. 825.
16. K. Shirai, J. Tani, T. Arai, M. Waturu, H. Takeda, T. Saegusa, "SCC evaluation test of a multi-purpose canister," *Proceedings, 13th International High-Level Radioactive Waste Management Conference (IHLRWMC)*, (American Nuclear Society, 2011): pp. 824-831.